buildings

MDPI

Article

A 4E Comparative Study between BIPV and BIPVT Systems in Order to Achieve Zero-Energy Building in Cold Climate

Ramtin Javadijam [1], Mohammad Hassan Shahverdian [1], Ali Sohani [2,*] and Hoseyn Sayyaadi [1]

[1] Lab of Optimization of Thermal Systems' Installations, Faculty of Mechanical Engineering-Energy Division, K.N. Toosi University of Technology, No. 15-19, Pardis Str., Mollasadra Ave., Vanak Sq., P.O. Box 19395-1999, Tehran 1999 143344, Iran; r.javadijam@email.kntu.ac.ir (R.J.); mohammadhassan.shahverdian@email.kntu.ac.ir (M.H.S.); sayyaadi@kntu.ac.ir (H.S.)

[2] Department of Enterprise Engineering, University of Rome Tor Vergata, Via Del Politecnico 1, 00133 Rome, Italy

* Correspondence: ali.sohani@uniroma2.it

Abstract: The growing demand for energy has led to the popularity of building integrated photovoltaic (BIPV) systems. However, photovoltaic (PV) system efficiency decreases as the temperature increases. To address this issue, a study was conducted on a BIPV thermal (BIPVT) system, which can generate both thermal and electrical energy, to enhance its efficiency. In this study, for the cold weather in Tabriz city in Iran, BIPV and BIPVT systems are compared with each other in terms of energy, economy, exergy, and environment (4E) and the goal is to fully supply the thermal and electrical load of the desired building. The studied criteria are electrical power and heat recovery, payback time (PBT), exergy efficiency, and saved carbon dioxide (SCD) from the energy, economic, exergy, and environmental point of view, respectively. Finally, it is concluded that in cold weather, the BIPVT system can achieve a 7.15% improvement in produced power compared to the BIPV system and 52.2% of the building's heating needs are provided. It also causes the exergy efficiency to improve by an average of 1.69% and saves 34.98 ton of carbon dioxide. The PBT of this study is calculated as 5.77 years for the BIPV system and 4.78 years for the BIPVT system.

Keywords: 4E analysis; net-zero building; building-integrated photovoltaic/thermal (BIPVT); cost effective technology; building façade

Citation: Javadijam, R.; Shahverdian, M.H.; Sohani, A.; Sayyaadi, H. A 4E Comparative Study between BIPV and BIPVT Systems in Order to Achieve Zero-Energy Building in Cold Climate. *Buildings* **2023**, *13*, 3028. https://doi.org/10.3390/buildings13123028

Academic Editor: Adrian Pitts

Received: 18 October 2023
Revised: 24 November 2023
Accepted: 26 November 2023
Published: 5 December 2023

1. Introduction

As a result of the increase in the global population, the need for energy has increased [1,2]. Environmental concerns and the reduction of fossil fuels have led policymakers to use renewable energy [3,4]. Renewable energy, particularly solar energy, has emerged as a crucial energy source on a global scale [5]. One of the most important technologies in the field of solar energy is photovoltaic (PV) cells [6]. These PV cells are able to convert solar energy into electrical energy [7,8].

Building integrated photovoltaic (BIPV) systems and building integrated photovoltaic thermal (BIPVT) systems are applications of these solar cells in the building [9]. BIPV systems have the ability to supply the electrical energy of the building [10], and BIPVT systems have the ability to supply thermal energy in addition to electrical energy [11,12]. These systems are able to provide part or even all the needs of a building [13]. In addition to reducing the use of non-renewable energy sources [14,15], these systems also help reduce air pollution [16] and are economical [17].

1.1. Literature Review

A part of the literature review is dedicated to BIPV systems. Liu et al. [18] examined the benefits of using BIPV systems in terms of energy supply and the aesthetic value of buildings. They analyzed various factors that influence the performance of BIPV systems at high solar radiation, such as module temperature, solar radiation, orientation, PV types, and inverter. The feasibility of BIPV systems in high irradiance was evaluated in terms of energy efficiency, environmental performance, and economic performance, while emphasizing an ideal coordination model for promoting BIPV system development. Finally, potential future research directions for BIPV systems in such regions were explored. Using the HOMER software, Rahmati and Jahangiri [19] examined the energy-economy-enviro potential of a BIPV system in Abadan. Sensitivity analysis considered factors like solar cell slope, azimuth, cloudiness, and system losses. Results indicated that the PV-grid system was the most cost-effective, with a positive azimuth angle being ideal after zero degrees. A slope of 30 degrees and azimuth angle of zero were found to generate electricity at USD 0.09 per kWh. They recommend using southwest-facing vertical walls with inclined PVs and windows for BIPV system implementation in Iran, hoping it assists architects and energy decision-makers. Gholami et al. [20] introduced a measurement that evaluates the potential of BIPV systems to meet the energy needs of buildings in Europe. According to their research, it was proposed that by maintaining a ratio of 0.78 for building skin to net surface area and a 30% ratio for building skin glazing, buildings in the EU could meet their electricity needs through BIPV systems by 2030. The study also highlights and examines eighteen obstacles and challenges that impede the widespread adoption of BIPV systems, categorized into decision-making, design, implementation, operation and maintenance, and end-of-life stages. Shirazi et al. [21] introduced a tool that evaluated the techno-economic aspects of PV installations in urban areas. It assisted policy-makers and investors in identifying suitable surfaces for PV installation based on energy production, economic footprint, and carbon footprint. The findings indicate that installing PV panels on building facades with optimal angles can increase energy production and internal rate of return by up to 19% and 6%, respectively, on south-facing facades. This tool offered architects and planning authorities a means to quantitatively assess solar planning decisions for buildings and urban areas. Kurz et al. [22] discussed the implementation of a photovoltaic system as a bicycle shed near a school building, serving as an example of a BIPV system that operated independently from the power grid. The study emphasized the importance of aligning energy consumption with production to avoid significant losses. It suggested using building automation to manage electricity production and consumption effectively. Additionally, the paper highlighted the potential distortion of real profits when using a fixed discount rate in financial analyses and proposes analyzing the NPV ratio with variable discount rates over the solar plant's entire lifespan.

Another part of the literature review is dedicated to BIPVT systems. Shakouri et al. [23] presented a study on the energy performance of a BIPVT double skin façade (BIPVT-DSF) in the Middle Eastern climate. They focused on reducing cooling and thermal loads and generating power over a year. By using an analytical model, the study demonstrated the potential for significant cooling load reduction and highlighted the benefits of implementing a BIPVT-DSF system. The findings suggested that such a system can reduce yearly cooling and thermal loads by 251.6 MWh and 17.8 MWh, respectively, while also improving the energy performance index of the building by 34.3%. The BIPVT system had been developed to generate electricity and hot water for various applications in Malaysia by Ibrahim et al. [24]. The system consisted of a high-efficiency PV module and a spiral flow absorber. The study analyzed the performance of the BIPVT system using energy and exergy analyses. The results showed that the PVT energy efficiency ranged from 55% to 62%, while the exergy efficiency of the PVT was lower at 12% to 14%. The system improved with higher solar radiation, reaching values between 98 and 404 W. The BIPVT system also achieved a primary energy-saving efficiency of 73% to 81%. Dash et al. [25] investigated different parameters to improve system efficiency and used a thermal model and mathematical analysis. The hybrid PVT system, considering both thermal and electrical energy, outperforms a regular PV system. By utilizing a soft computing technique, the system's exergy was optimized by adjusting air velocity and channel length. The proposed system achieved significant gains in both thermal energy (54.7 MWh) and electrical energy

(15.8 MWh). Zhao et al. [26] examined the performance of an air-type BIPVT system in different environmental conditions. Using movable experimental systems with the new generation of photovoltaic modules, experiments were conducted in four cities with varying latitudes. The study investigated the relationship between climate conditions and the system's photothermal, flow rate, and photovoltaic performance. Results showed that thermal energy and power generation were positively correlated with irradiation intensity. Increasing the flow rate improved thermal energy, but had minimal impact on electrical efficiency. Regional comparisons revealed significant variations in thermal efficiency at high flow rates, while power generation remained relatively consistent. These findings can inform the design of air-type BIPVT systems.

Shahsavar et al. [27] made a comparison between a hybrid BIPVT system and an earth–air heat exchanger (EAHE), as well as their individual counterparts. The analysis included various aspects such as energy, exergy, environmental, exergoeconomic, and enviroeconomic factors. The hybrid system had the ability to regulate outdoor air temperature in both winter and summer while generating electricity. The results showed that the hybrid system outperforms the individual BIPVT and EAHE systems, producing higher yearly thermal and electrical energies by approximately 10.1% and 935.6%, respectively. However, the hybrid system had slightly lower yearly thermal and electrical exergy compared to the BIPVT system. Dash et al. [28] presented an analysis of the BIPVT system, specifically focusing on solar cell tile arrays and semitransparent arrays. The analysis showed that a semitransparent BIPVT system outperforms other systems in terms of energy effectiveness and exergy. A semitransparent BIPVT system achieved a higher energy gain of 2.5 kWh compared to solar cell tile arrays. The electrical efficiency was enhanced to 17.17% from 16%, and the overall exergy increases to 18.4% from 17.1%, representing growth of 6.8% and 7.6%, respectively. Ren et al. [29] introduced a novel BIPVT module that utilizes a micro heat pipe array, proposing the concept of a BIPVT near-zero-energy building. They also suggested a multi-energy complementary energy supply system for this building. The study employed TRNSYS to develop models for both the building and the energy supply system. By analyzing the heat transfer process of BIPVT components, the study aimed to understand the load characteristics of BIPVT buildings. The evaluation index for near-zero-energy buildings was utilized to calculate the energy-saving rate. The results indicated that BIPVT buildings exhibit 8.6% higher cooling and heating loads compared to benchmark buildings. However, the BIPVT building demonstrated a 32.3% reduction in annual cumulative energy consumption, with the system supplying 61.2% of the required energy. The energy consumption index for the BIPVT building was measured at 70.26 $kWh{\cdot}m^{-2}$, signifying a 76.6% energy saving rate and a 32.3% enhancement in energy efficiency compared to the benchmark building.

Bot et al. [30] presented an experimental study of a BIPVT system for heat recovery in a test room. The focus was on presenting the measured values that represented the main boundary (room and weather characteristics) conditions and the thermal behavior and performance of the BIPVT system. The system was located in the Solar Building, which is a nearly zero-energy building exposed to the Mediterranean climate conditions of Portugal. Lamnatou et al. [17] presented a Life Cycle Assessment (LCA) study that evaluated the environmental impact of a BIPVT system developed at a university. The study tested material manufacturing and analyzed various environmental indicators such as cumulative energy demand and ecological footprint and global warming potential. The results highlighted the significant impact of PV cells and steel components. The recycling of steel was found to reduce the impact by 47% to 85%. They also calculated the impact per square meter of thermal absorber and discussed factors influencing the BIPVT system environmental profile, including storage materials and end-of-life management. Luo et al. [31] investigated different building envelope systems integrating PV, TE modules, energy storage, and control algorithms. These systems helped to reduce thermal load in buildings and provide cooling/heating supply. Each system had an optimal thermal energy load, resulting in minimal annual power consumption. Except for one system, the others achieved negative accumulated power consumption, effectively reducing the thermal load to zero. Shakouri et al. [32] investigated the 4E aspects of a BIPVT system in an existing office building. Different scenarios with varying glass windows and PV module surface areas were evaluated. The results suggested a scenario with the lowest PV module surface area and highest glass window area for improved energy efficiency and lowest initial investment. Additionally, a scenario with the highest PV module area and zero glass windows was recommended for maximum energy generation, emission reduction, and revenue. A retrofit measure with the highest PV module surface area and a payback period of 1.58 years was proposed based on the analysis.

1.2. Research Gap and Novelty

Despite the important and valuable studies that were observed in the literature review, there are still some gaps that can be answered. In most studies, the use of one of the BIPV or BIPVT systems has been evaluated or modeled from different perspectives.

Consequently, the novelty of the present study is the comparison of two, BIPV and BIPVT, systems from different perspectives. The purpose of the energy perspective in the current study is to compare the produced electrical energy of the BIPV and BIPVT systems as well as the heat recovery of the BIPVT system. The electrical and thermal exergy efficiencies have been selected from the exergy point of view to compare the two systems. Payback time (PBT) is an important economic parameter to compare these two systems, and the amount of saved carbon dioxide (SCD) has also been chosen from an environmental point of view so that the performance of these two systems can be compared.

1.3. Outline

This study consists of five parts under the titles of introduction, case study, modeling, results and conclusion, respectively.

2. Case Study

In this part of the study, the investigated building, the investigated city, and the thermal and electrical loads of the building are discussed.

2.1. The Investigated Building

The building investigated in this section is residential, with six floors and two units on each floor. More details related to the heat transfer coefficient are given in Table 1.

Table 1. U-Value of different parts ($W{\cdot}m^{-2}{\cdot}K^{-1}$) [33].

Item	Description
Internal Wall	1.42
External wall	1.01
Windows	2.8
Roof	0.6
Floor	0.67

2.2. The Investigated City

Tabriz is considered as the investigated city in this research. Tabriz is a metropolis located in the northwest of Iran. The climate of this city is extremely cold in the winter and temperate in the summer. Other specifications are given in Table 2.

Table 2. Information on Tabriz [33].

City	Summer Category	Summer		Winter Category	Winter	Lat (°N)	Lon (°E)
		Tdb (°C)	Twb (°C)		Tdb (°C)		
Tabriz	Temperate	34.0	18.0	Relative cold	−10.8	37.8	46.3

The primary goal of installing a BIPVT system is to recover heat using the air flowing in the airgap between PV and walls. The recovered heat is then utilized for space heating purposes. The secondary goal of installation is to reduce the working temperature of PV. Therefore, this study was performed using a cold city, since as the main goal of the installation of a BIPVT system, the system was employed to provide part of the heating load and reduce the amount of required fuel for the fossil-fuel-burning conventional heating system. Providing part of the space heating using a BIPVT system has considerable energy and economic benefits. It also leads to decreased environmental effects compared to the complete heating load provision by the conventional fossil-fuel-burning system. The colder a city is, the higher the indicated benefits are.

2.3. Electrical and Heating Load

The electrical load required for the given building in Tabriz city is given in Figure 1. A sample day which is in the middle of each month is shown in the figures. To enhance visualization, the information is presented for a single day in each month, resulting in a total of 288 h for the entire year. This calculation is derived from multiplying the number of hours in a sample day (24) by the number of months in a year (12). The amount of required electrical load is higher during the hours when the sun is not in the sky, as shown in Figure 1.

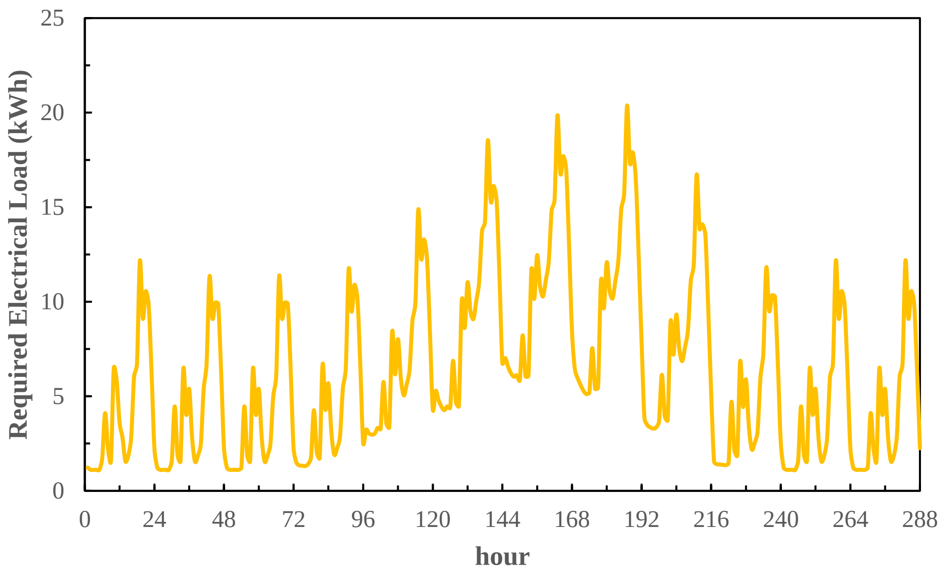

Figure 1. Required electrical load.

The required thermal load of the building is also given in Figure 2. The amount of heat load is higher in the cold months of the year and this amount is close to zero in the hot months of the year. Like the electrical load, the amount of thermal load is also higher at night, as shown in Figure 2.

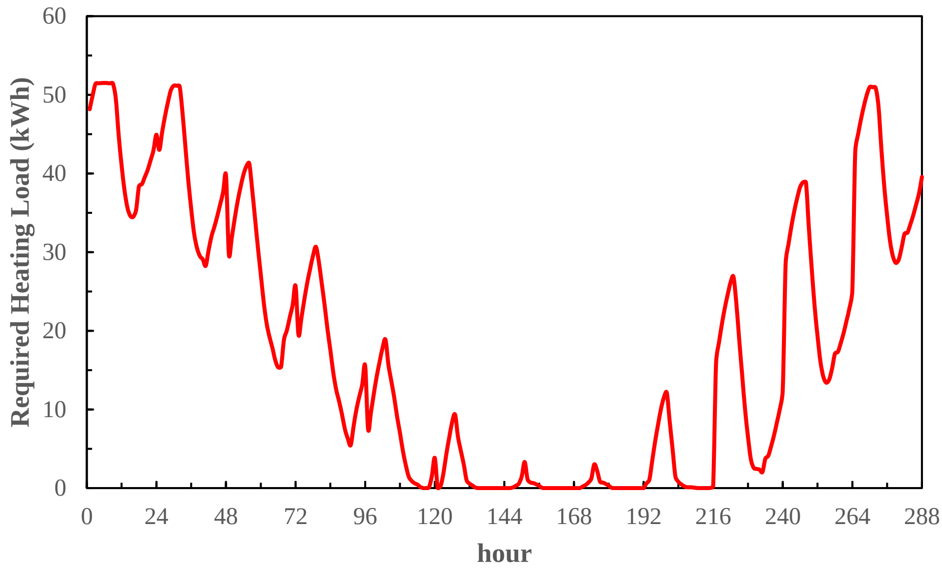

Figure 2. Required heating load.

3. Modeling

In this section, the system under review is presented first. As can be seen in Figure 3, the investigated system in one scenario is the BIPV system and in the second scenario it is the BIPVT system. In the following part, the studied system is modeled from energy, exergy, economic, and environmental perspectives.

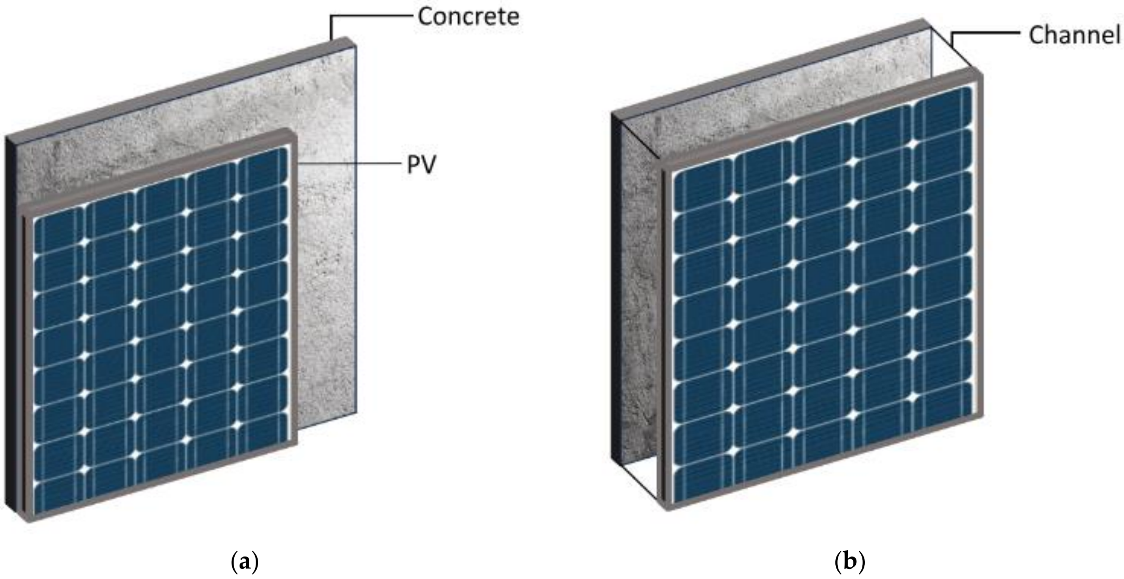

Figure 3. Studied system: (**a**) BIPV; (**b**) BIPVT.

3.1. Energy Analysis

A photovoltaic solar cell consists of five layers of glass, top EVA, silicon, bottom EVA, and Tedlar. In the BIPV system, this solar cell is integrated with the building and the BIPVT system adds an air channel layer to the system. The equations of the different layers of the BIPVT system are given below, and for the BIPV system, it is enough to remove the air channel layer [34,35].

$$c_{p,g}\delta_g A\rho_g \frac{dT_g}{dt} = \alpha_g GA + \frac{T_{EVA1} - T_g}{R_{cond,EVA1,g}} - \frac{T_g - T_a}{R_{conv-g,a}} - \frac{T_g - T_{sky}}{R_{rad-g,sky}} \tag{1}$$

$$c_{p,EVA1}\delta_{EVA1}A\rho_{EVA1}\frac{dT_{EVA1}}{dt} = \frac{T_{Si}-T_{EVA1}}{R_{cond,Si,EVA1}} - \frac{T_{EVA1}-T_g}{R_{cond,EVA1,g}} \tag{2}$$

$$c_{p,si}\delta_{si}A\rho_{si}\frac{dT_{si}}{dt} = \alpha_{si}\tau_g GA - P - \frac{T_{si}-T_{EVA1}}{R_{cond,si,EVA1}} - \frac{T_{si}-T_{EVA2}}{R_{cond,EVA2,si}} \tag{3}$$

$$c_{p,EVA2}\delta_{EVA2}A\rho_{EVA2}\frac{dT_{EVA2}}{dt} = \frac{T_{Si}-T_{EVA2}}{R_{cond,EVA2,Si}} - \frac{T_{EVA2}-T_{Td}}{R_{cond,EVA1,Td}} \tag{4}$$

$$c_{p,Td}\delta_{Td}A\rho_{Td}\frac{dT_{Td}}{dt} = \frac{T_{EVA2}-T_{Td}}{R_{cond,EVA2,Td}} - \frac{T_{Td}-T_{ac}}{R_{conv-Td,ac}} - \frac{T_{Td}-T_c}{R_{rad-Td,c}} \tag{5}$$

in which c_p, δ, ρ, A, T, and t are specific heat capacity, thickness, density, area, temperature, and time. α, τ, G, P, and R are absorptivity, transmittivity, radiation, produced power, and thermal resistance. The 5 layers of introduced solar cells are displayed from top to bottom by g, $EVA1$, Si, $EVA2$, and Td indices, ac and c indices belong to the air channel and concrete. Three types of conductive, convective, and radiant heat transfer are also displayed with $cond$, $conv$, and rad indices.

The thermal resistance associated with each type of heat transfer has its own equation. In Equation (6), the thermal resistance related to conductive heat transfer is observed [36].

$$R_{cond-i,j} = \frac{\delta_i}{2k_iA_i} + \frac{\delta_j}{2k_jA_j} \tag{6}$$

where k is thermal conductivity and the two indices i and j are related to two different layers. In Equation (7), the thermal resistance related to convective heat transfer between glass and air is observed [36].

$$R_{conv-g,a} = \frac{1}{(2.8+3V_w)A} \tag{7}$$

In Equation (8), the thermal resistance of convective heat transfer between the Tedlar layer and the air channel is given [37].

$$R_{conv-Td,ac} = \frac{D_h}{Nuk_{ac}A} \tag{8}$$

in which D_h and Nu are hydraulic diameter and Nusselt number, respectively. The Nusselt number related to air in the channel is calculated by Equation (9) [35].

$$Nu = \begin{cases} 3.66 & \mathrm{Re} < 2300 \\ 0.023\mathrm{Re}^{0.8}\mathrm{Pr}^{0.4} & \mathrm{Re} \geq 2300 \end{cases} \tag{9}$$

where Re and Pr are Reynolds and Prandtl number, respectively. In Equation (10), the thermal resistance of radiative heat transfer is given [34].

$$R_{rad-i,j} = \frac{1}{\sigma\varepsilon_i A(T_i^2+T_j^2)(T_i+T_j)} \tag{10}$$

in which ε and σ are emissivity and Stefan–Boltzmann, respectively.

The next energy balance equation is related to the air channel layer, which is given in Equation (11) [38].

$$c_{p,ca}\delta_{ca}A\rho_{ca}\frac{dT_{ca}}{dt} = Q_{flow} - \frac{T_c-T_{ac}}{R_{conv-c,ac}} + \frac{T_{Td}-T_{ac}}{R_{conv-Td,ac}} \tag{11}$$

where [38]

$$Q_{flow} = \dot{m}_{ca}c_{p,ca}(T_{inlet}-T_{ca}) \tag{12}$$

where $\dot{m}_{ca}$ and T_{inlet} are mass flow rate and inlet temperature of air in channel.

The last layer is related to concrete, whose energy equation is shown in Equation (13) [39].

$$c_{p,c}\delta_c A\rho_c \frac{dT_c}{dt} = \frac{T_c - T_{ac}}{R_{conv-c,ac}} + \frac{T_{Td} - T_c}{R_{rad-Td,c}} + \frac{T_c - T_{room}}{R_{cond,c,room}} \quad (13)$$

T_{room} is the thermal comfort temperature of the room. According to the identification of the energy balance equations for each layer, the electric power is obtained according to Equation (14) [40].

$$P = \eta_{ref}\left(1 - \beta_{ref}\left(T_{si} - T_{ref}\right)\right)GA \quad (14)$$

where η_{ref} and β_{ref} are the reference efficiency and temperature coefficient of the BIPV system.

Also, the heat recovery in the BIPVT system is obtained according to Equation (15) [27].

$$\dot{Q}_h = \dot{m}_{ca}c_{p,ca}\left(T_{outlet} - T_{inlet}\right) \quad (15)$$

where T_{outlet} is outlet temperature from the air channel.

The constant values of parameters related to energy modeling in this research are listed in Table 3.

Table 3. Specifications of the system [37,39,41].

Parameters		Unit	Value
Efficiency at Reference		%	14
Reference Temperature		°C	25
Temperature Coefficient of PV		$\%\cdot(°C)^{-1}$	0.43
Thickness of	Glass	mm	3.2
	Top EVA	mm	0.5
	Silicon	mm	0.4
	Bottom EVA	mm	0.5
	Tedlar	mm	0.33
	Wall	mm	0.3

3.2. Exergy Analysis

In this part, the modeling of three important exergy parameters, i.e., electrical, thermal, and net exergetic efficiency, are discussed. In the BIPV system, thermal exergetic efficiency is not defined, due to having only power generation and no heat recovery, and the electrical efficiency is equal to the overall efficiency, but in the BIPVT system, the three mentioned efficiencies can be calculated [42].

The net exergetic efficiency in the system is obtained according to Equation (16) [43].

$$\varepsilon_{net} = \frac{E_x^P + E_x^Q}{E_x^{sun}} \quad (16)$$

in which E_x^P, E_x^Q, and E_x^{sun} are exergy of power, heat, and sun. Exergy of power is calculated according to Equation (17) [44].

$$E_x^P = P \quad (17)$$

Exergy of heat is obtained according to Equation (18) [44].

$$E_x^Q = Q_h\left(1 - \frac{T_a}{T_{outlet}}\right) \quad (18)$$

Exergy of sun is calculated from Equation (19) [35].

$$E_x^{sun} = GA\left[1 - \frac{4}{3}\left(\frac{T_a}{T_{sun}}\right)\right] \quad (19)$$

where T_{sun} is sun temperature.

Finally, to calculate the exergetic efficiency in electrical and thermal parameters, two equations, Equations (20) and (21), can be used [45].

$$\varepsilon_{ele} = \frac{E_x^P}{E_x^{sun}} \quad (20)$$

$$\varepsilon_{th} = \frac{E_x^Q}{E_x^{sun}} \quad (21)$$

3.3. Economic Analysis

The economic analysis conducted for this research included obtaining the payback time (PBT) for the BIPV and BIPVT systems. In the BIPV system, with initial costs and operating and maintenance costs, a profit is made by selling electricity, but in the BIPVT system, profit is obtained by selling electricity and thermal energy.

PBT in the BIPV system is calculated according to Equation (22).

$$\frac{AGE \times c_{ele}(1+i_{elec})^{PBT-1}}{(1+d)^{PBT}} - IC - \frac{f \times IC(1+i_{om})^{PBT-1}}{(1+d)^{PBT}} = 0 \quad (22)$$

where AGE is annual generated electricity and IC is initial cost. i and d are inflation and discount rate, respectively. The subtitles of $elec$ and om are equal to electricity and operating and maintenance, respectively. c_{ele} is the cost of electricity and f is a constant value and is equal to a percentage of the initial costs.

PBT in the BIPVT system is calculated according to Equation (23) [40].

$$\frac{AGE \times c_{elec} \times (1+i_{elec})^{PBT-1}}{(1+d)^{PBT}} + \frac{\frac{AGH}{\eta_{heating\ system}} \times \left(\frac{1}{LHV_{NG}}\right) \times \rho_{NG} \times c_{NG} \times (1+i_{NG})^{PBT-1}}{(1+d)^{PBT}} - IC - \frac{f \times IC \times (1+i_{OM})^{PBT-1}}{(1+d)^{PBT}} = 0 \quad (23)$$

in which AGH is annual generated heat. The subtitle NG is equal to natural gas. LHV is low heat value and $\eta_{heating\ system}$ is the efficiency in the heating system and ρ_{NG} is the density of natural gas.

The economic characteristics used in this research for both BIPV and BIPVT systems are listed in Table 4.

Table 4. Economic parameters [8,40,46].

Symbol	Unit	Value
c_{elec}	$\$\cdot(\text{kWh})^{-1}$	0.28
i_{elec}	%	7
c_{NG}	$\$\cdot\text{m}^{-3}$	0.07
i_{NG}	%	3
$\eta_{heating\ system}$	%	60
i_{OM}	%	2
d	%	2

3.4. Environmental Analysis

The environmental analysis carried out in this section for the two, BIPV and BIPVT, systems include the amount of saved carbon dioxide that was not released into the environment.

The amount of SCD in power generation by the BIPV and BIPVT systems is obtained according to Equation (24) [40].

$$SCD_{elec} = pcd_{elec} \times GE \quad (24)$$

in which GE is generated electrical energy and pcd_{elec} is the amount of CO_2 produced for the produced power process in the thermal power plant. Due to the use of the solar system, there is no need to produce power by the thermal power plant, and for that amount of energy produced, a certain amount of carbon dioxide in the environment is not published. According to reference [40], for electricity produced in a thermal power plant, pcd_{elec} is equal to 0.598 kg per kilowatt hour of produced electrical energy.

The amount of SCD in heat generation using the BIPVT system is obtained according to Equation (25) [40].

$$SCD_{heat} = pcd_{NG} \times \frac{HR}{\eta_{heating\ system}} \tag{25}$$

where HR is heat recovery and pcd_{NG} is the produced carbon dioxide per burning unit of natural gas, which according to the reference [40] will be equal to 0.185 kg per kWh of consumed natural gas.

3.5. Calculation Procedure

To clarify the modeling process, the solution process is shown in Figure 4. For this purpose, weather information and physical and structural properties are considered first, and in the next step, by solving the energy equations of each layer, the power and heat produced at any time are obtained.

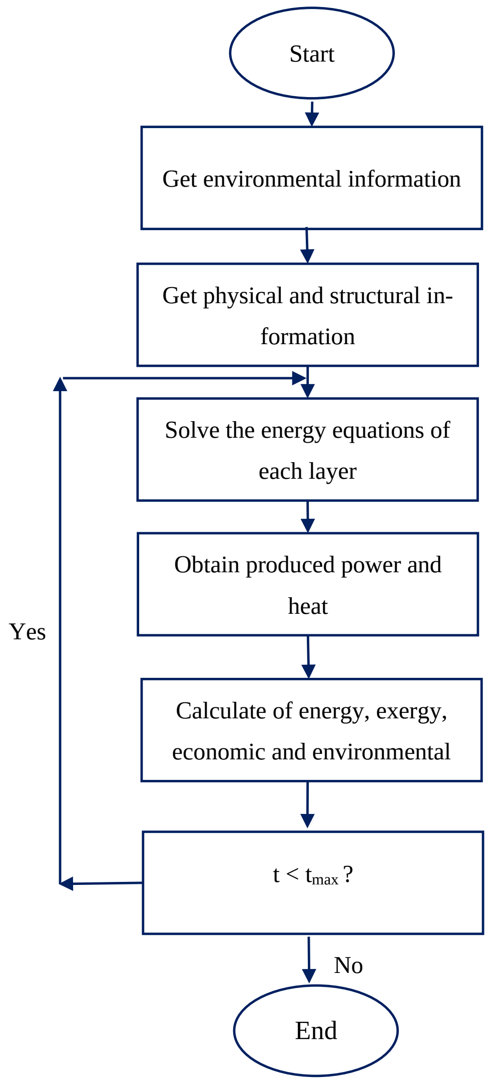

Figure 4. Calculation procedure.

The potential error might come from the uncertainty in the input parameters like the weather characteristics or load profile. However, as the weather data comes from the average during the past years, it would have low uncertainty. In addition, the uncertainty for the load profile might come from some assumptions like the number of people in the place at a certain time. Nonetheless, such assumptions do not have a considerable impact on the obtained loads.

4. Results

In this section, the results of the modeling from the previous section are given. In the first part, the BIPVT system validation is presented. In the next section, the modeling results from energy, exergy, economic, and environmental perspectives are given.

4.1. Model Validation

To ensure the modeling results, in this part, the model validation is presented. The BIPVT system modeling results have been validated using a reference. The modeling results are shown in Figure 5. It is worth noting that for validation, the climate data and system specifications in the reference [39] and the present study have been unified.

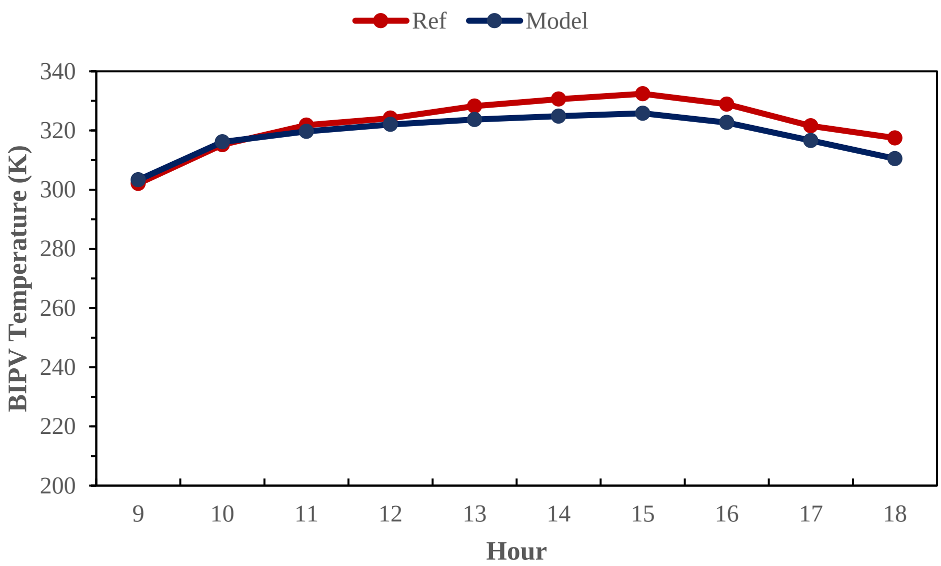

Figure 5. BIPVT system validation.

Based on Figure 5, only a 1.28% difference from the reference [39] is observed in the BIPVT system temperature prediction, which can be trusted in the modeling results due to the low difference.

4.2. Modeling Results

The results obtained from the mathematical modeling section are given in this part. The energy, exergy, economy, and environment results are given in this part, respectively.

4.2.1. Energy Results

The results related to the produced energy associated with the BIPV and BIPVT systems are given in this part. The diagram of hourly electrical energy produced by the two studied systems is given in Figure 6.

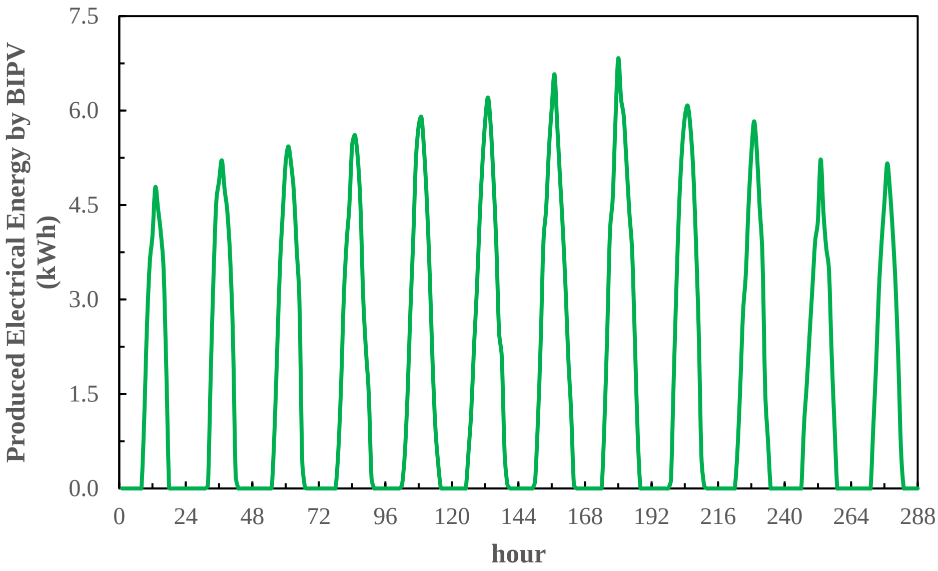

(**a**)

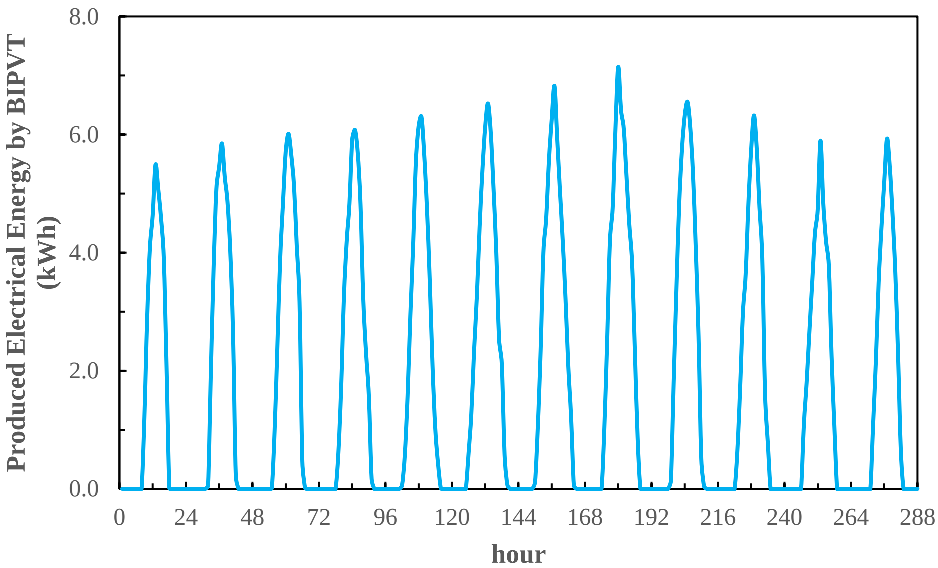

(**b**)

Figure 6. Hourly produced electrical energy: (**a**) BIPV; (**b**) BIPVT.

As shown in Figure 6, the produced electrical energy at different hours of the day is known for each month (in the middle of each month), so that during the day, as the radiation increases, the produced power also increases, and at sunset, this amount decreases to zero again. At noon, the amount of electrical power is the highest in every month. For example, in the month of January at 12 o'clock, the amount of electrical energy produced for the BIPV and BIPVT systems is 4 and 4.6 kWh, respectively, and the BIPVT system produces 15% more electrical energy than the BIPV system at this particular time. For a better comparison, the monthly graph of the produced electrical energy is given in Figure 7.

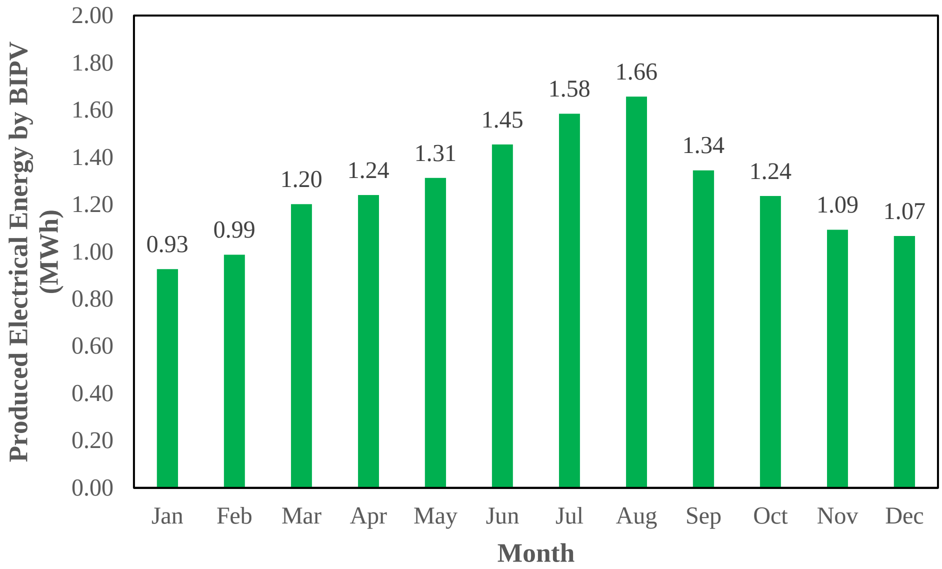

(**a**)

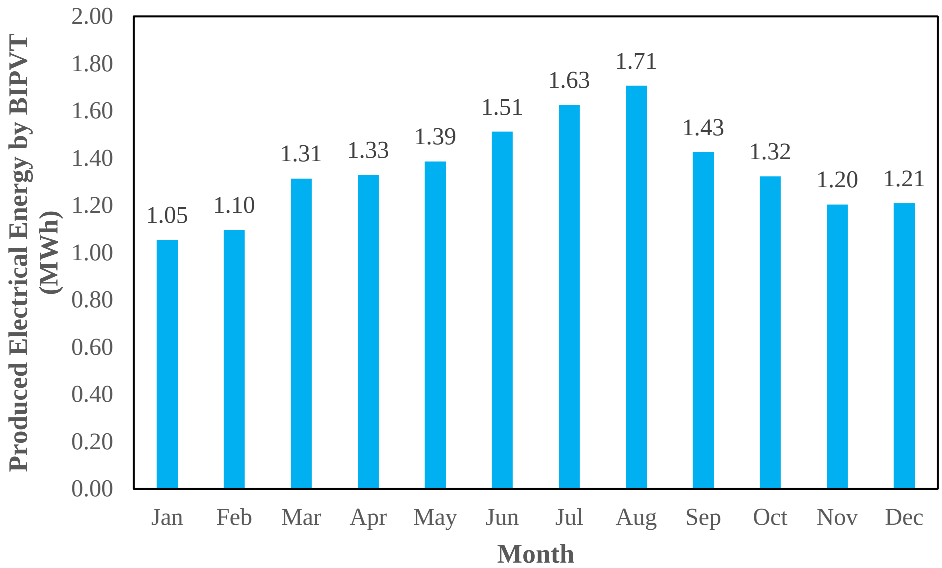

(**b**)

Figure 7. Monthly produced electrical energy: (**a**) BIPV; (**b**) BIPVT.

According to Figure 7, the amount of produced electrical energy in the hot months of the year, when the radiation and hours of the sun are more in those months, is higher, and in the cold months of the year, the amount of produced electrical energy is less and this procedure is similar for BIPV and BIPVT systems. For example, in the BIPV and BIPVT systems, the highest production of electrical energy is in the month of August and is equal to 1.66 and 1.71 MWh, and the lowest electrical energy production is related to the month of January, which is equal to 0.93 and 1.05 MWh. According to the figure, the electrical energy produced in the BIPVT system is more than produced in the BIPV system, which is clearly shown in Figure 8.

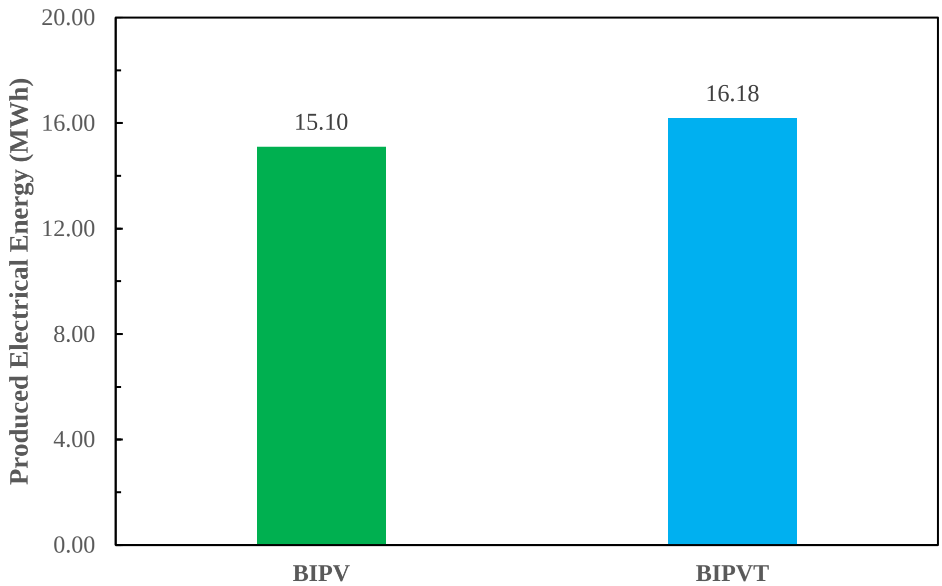

Figure 8. Yearly produced electrical energy.

Based on Figure 8, the electrical energy produced by the BIPV system is 15.10 MWh, and for the BIPVT system this value is equal to 16.18 MWh, which is 1.08 MWh more. As a result, by using the air channel behind the photovoltaic solar system, the produced electrical energy can be increased by 7.15%.

As stated in the introduction, the advantage of the BIPVT system compared to BIPV is the ability to produce thermal energy. The monthly thermal energy produced by the BIPVT system is given in Figure 9.

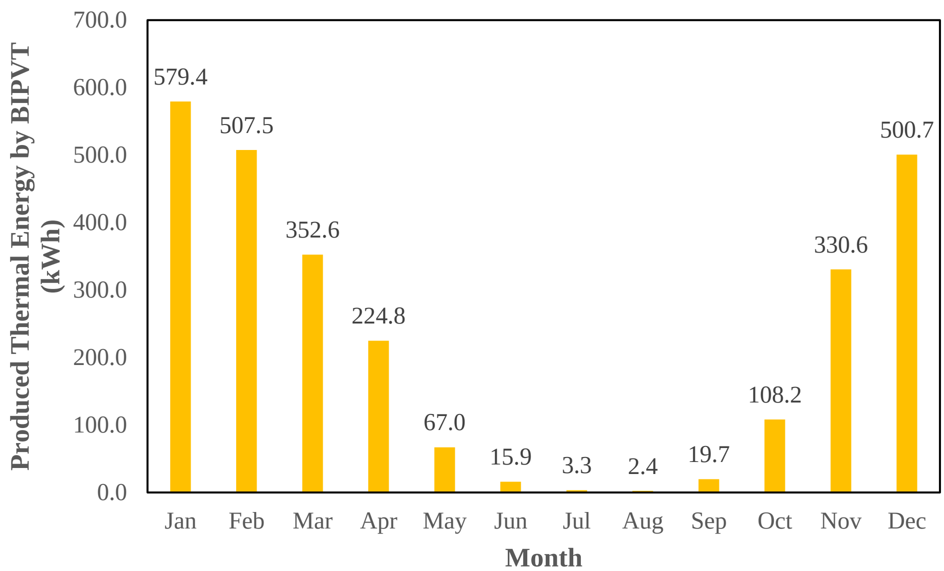

Figure 9. Monthly produced thermal energy.

It is expected that the produced thermal energy is more in the hot months, considering that there is no need for thermal energy in these months. This means that despite the production of thermal energy in the hot months of the year in the BIPVT system, due to the high ambient temperature, the produced heat is not needed, and only the required amount is shown in Figure 9. It is not shown in Figure 9. The highest thermal energy production is associated with the month of January, and is equal to 579.4 kWh.

Figure 10 shows the annual produced thermal energy production.

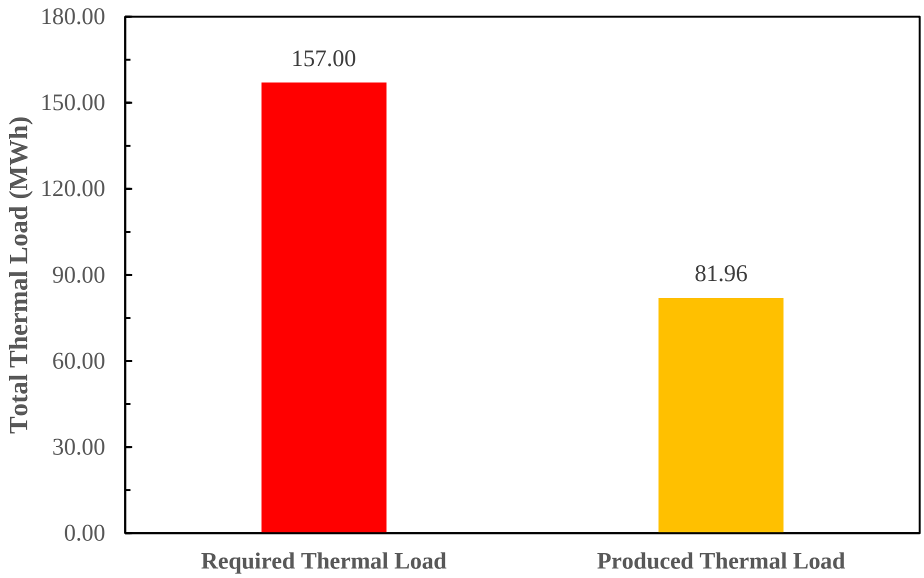

Figure 10. Yearly produced thermal energy.

The amount of thermal energy produced per year is equal to 81.96 MWh and the total amount of required load per year is equal to 157.00 MWh. As a result, the BIPVT system has the ability to supply 52.2% of the required thermal load. In the next section, the exergy efficiency in the two investigated systems is compared.

4.2.2. Exergy Results

Exergy analysis allows for the detection of energy loss within an energy system and offers a precise assessment of the usable work that can be extracted from the system. In this study, exergy efficiency was investigated. In the BIPV system, electrical exergetic efficiency was investigated, and in the BIPVT system electrical and thermal exergetic efficiency were investigated.

Figure 11 shows the electrical exergetic efficiency in the BIPV system at different times of the year.

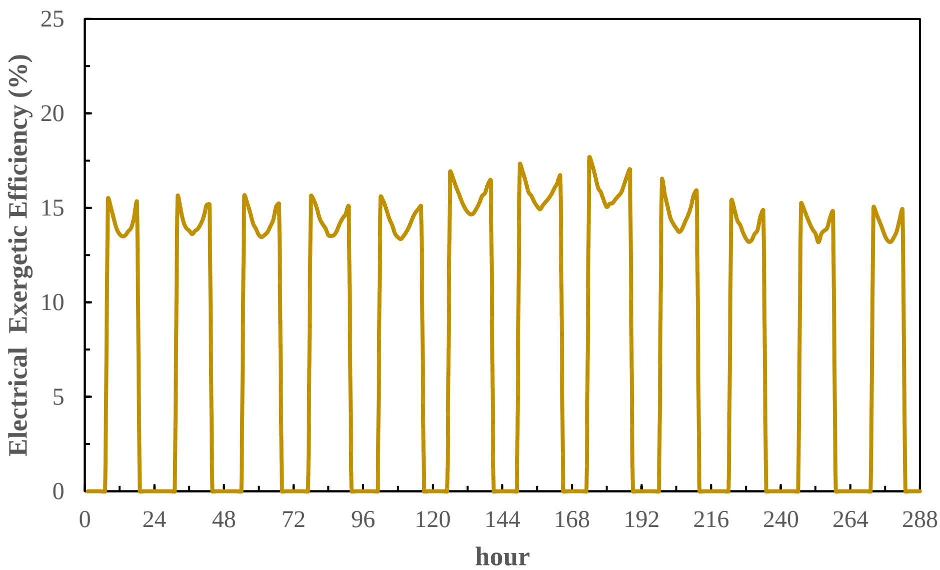

Figure 11. Electrical exergetic efficiency.

Based on Figure 11, the exergy efficiency is zero in the hours when the sun is not in the sky, and the exergy efficiency increases when the sun rises. The amount of exergy efficiency at noon is lower compared to other hours, which is due to the high radiation of the sun and the inability of the solar system to convert it into electrical power. For example, in February at 9:00 a.m., it is 14.95% and at 1:00 p.m. this value reaches 13.6%.

The exergy efficiencies related to power, heat, and total exergetic efficiency for the BIPVT system are given in Figure 12.

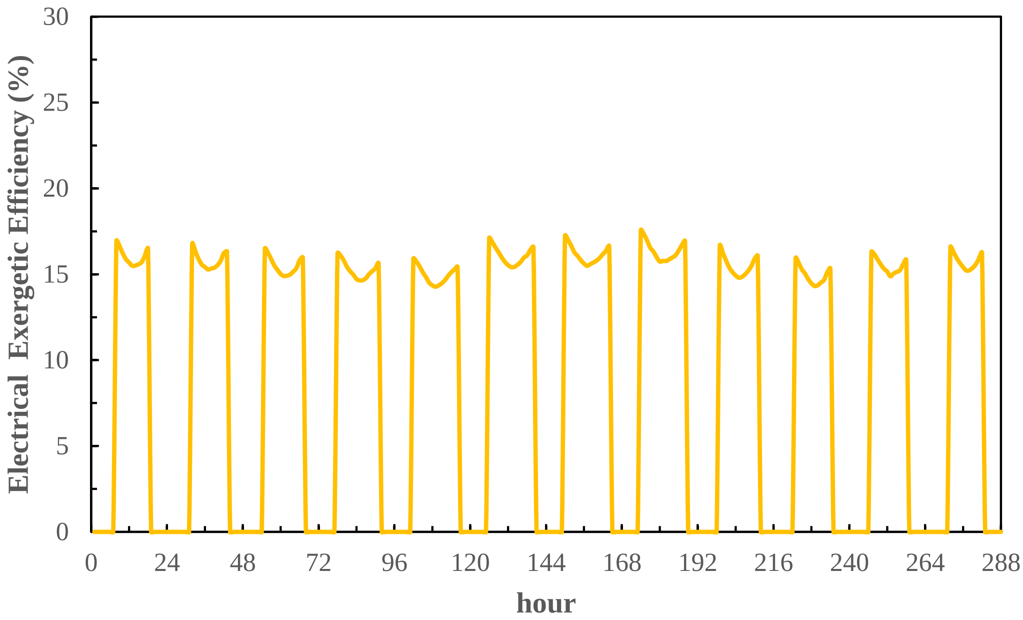

(**a**)

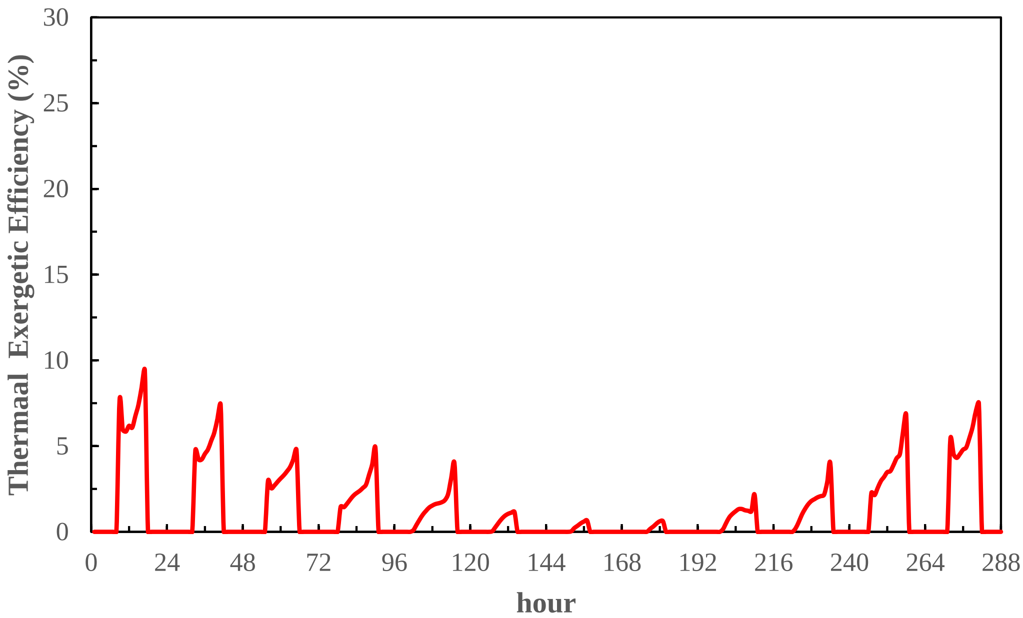

(**b**)

Figure 12. *Cont.*

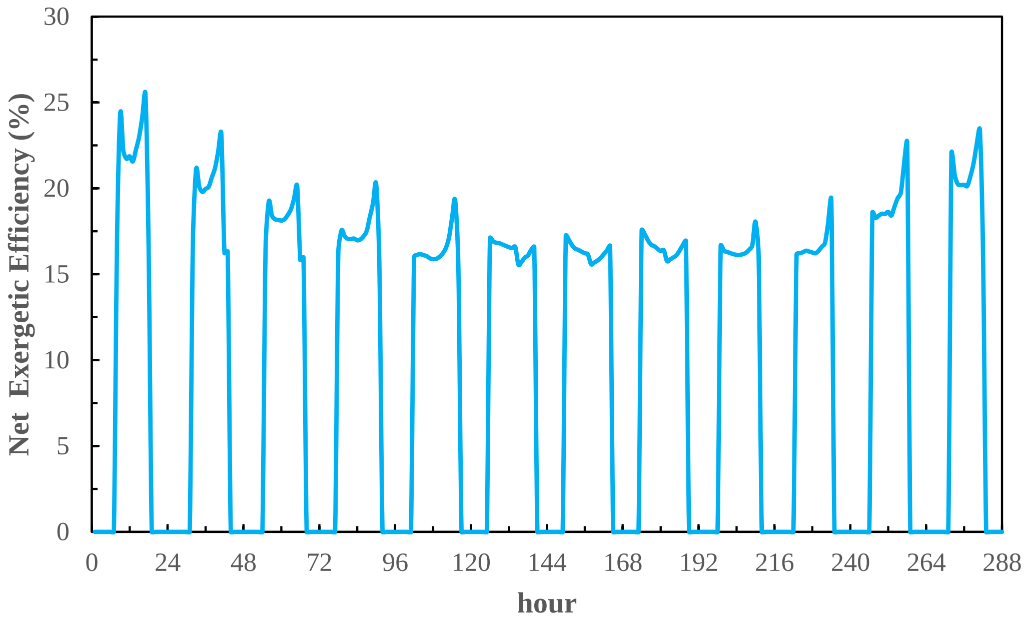

(**c**)

Figure 12. Exergetic efficiency for the BIPVT system: (**a**) electrical; (**b**) thermal; (**c**) net.

According to Figure 12, the procedure of electrical exergetic efficiency in the BIPVT system is similar to BIPV system with the difference that the electrical exergetic efficiency in the BIPVT system is higher than that of the BIPV system, which is due to the higher production power of the BIPVT system. For example, in the month of February and at nine and thirteen, the electrical exergy efficiency is 16.77 and 15.28%, respectively, which is 1.82% and 1.68% different from the BIPV system.

The thermal exergetic efficiency has meaning during the hours of the sun, as does the electrical exergetic efficiency. Thermal energy efficiency at noon is lower than in the afternoon. The reason is that the solar radiation decreases significantly in the afternoon, but the temperature of the solar cell surface takes time to decrease and it still has a good performance in generating thermal energy. As a result, the efficiency in the solar cell increases significantly. For example, in February at 13:00 and 16:00, the value of thermal exergetic efficiency is 4.81% and 6.59%, respectively.

In the case of total exergy efficiency, this value is equal to the sum of thermal and electrical exergy efficiency. For example, in the month of February at 1 p.m., the total efficiency value is 20.09%.

4.2.3. Economic Results

By determining the amount of energy produced in each system, the two systems should be compared from an economic point of view. Figure 13 compares the PBT of BIPV and BIPVT systems.

As can be seen, the PBT of the BIPV system is equal to 5.77 years and the PBT of the BIPVT system is equal to 4.78 years. The reason for this being lower is due to more produced power in the BIPVT system and to produced heat, which caused the PBT to decrease by 0.99 years. Figure 14 shows the cash flow for the BIPVT system.

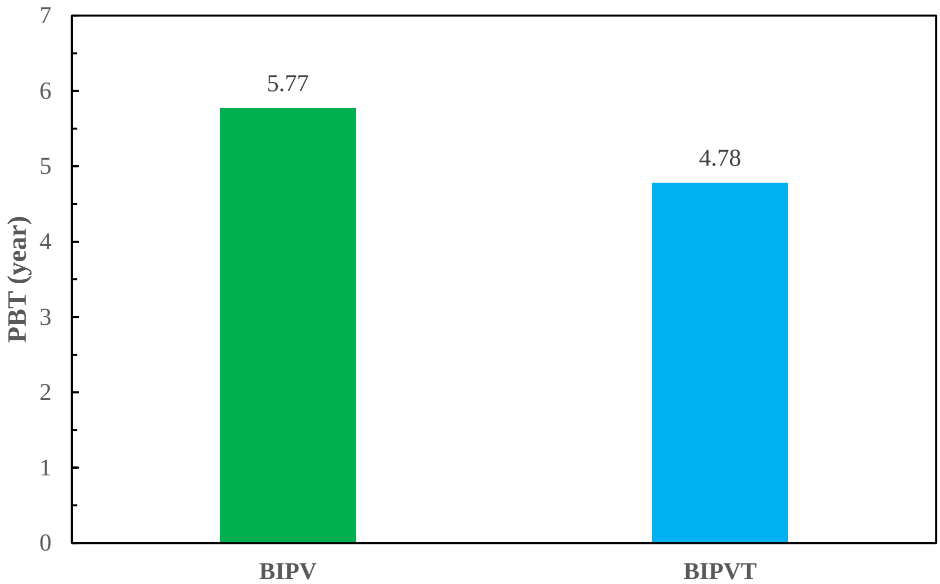

Figure 13. PBT of the systems.

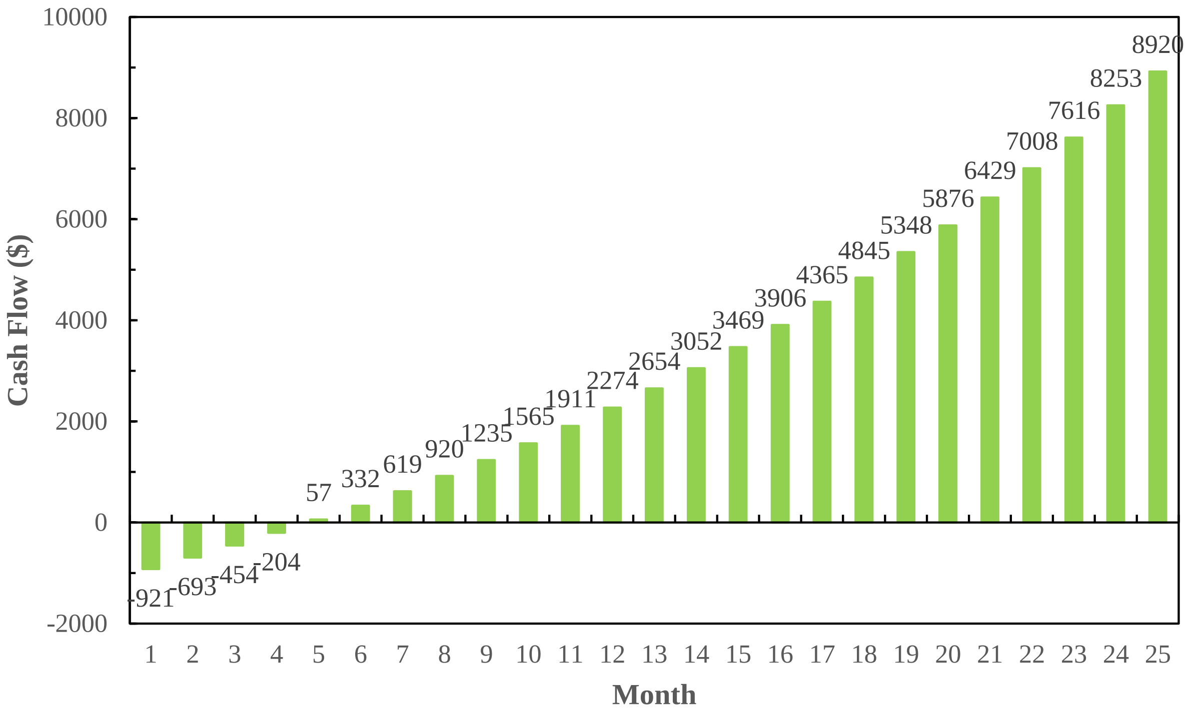

Figure 14. Cash flow of the BIPVT system.

In the first year, the amount of cash flow is equal to USD −921 and it increases annually until it reaches USD −204 in the fourth year and reaches USD 57 in the 5th year. This change of sign shows that the PBT has happened, which is 4.78 years in the BIPVT system. In the last year of life, the 25th year, the amount of cash flow reaches USD 8920.

4.2.4. Environmental Results

The next important parameter that was investigated is the amount of saved carbon dioxide. Figure 15a shows this value for the BIPV system and Figure 15b for the BIPVT system.

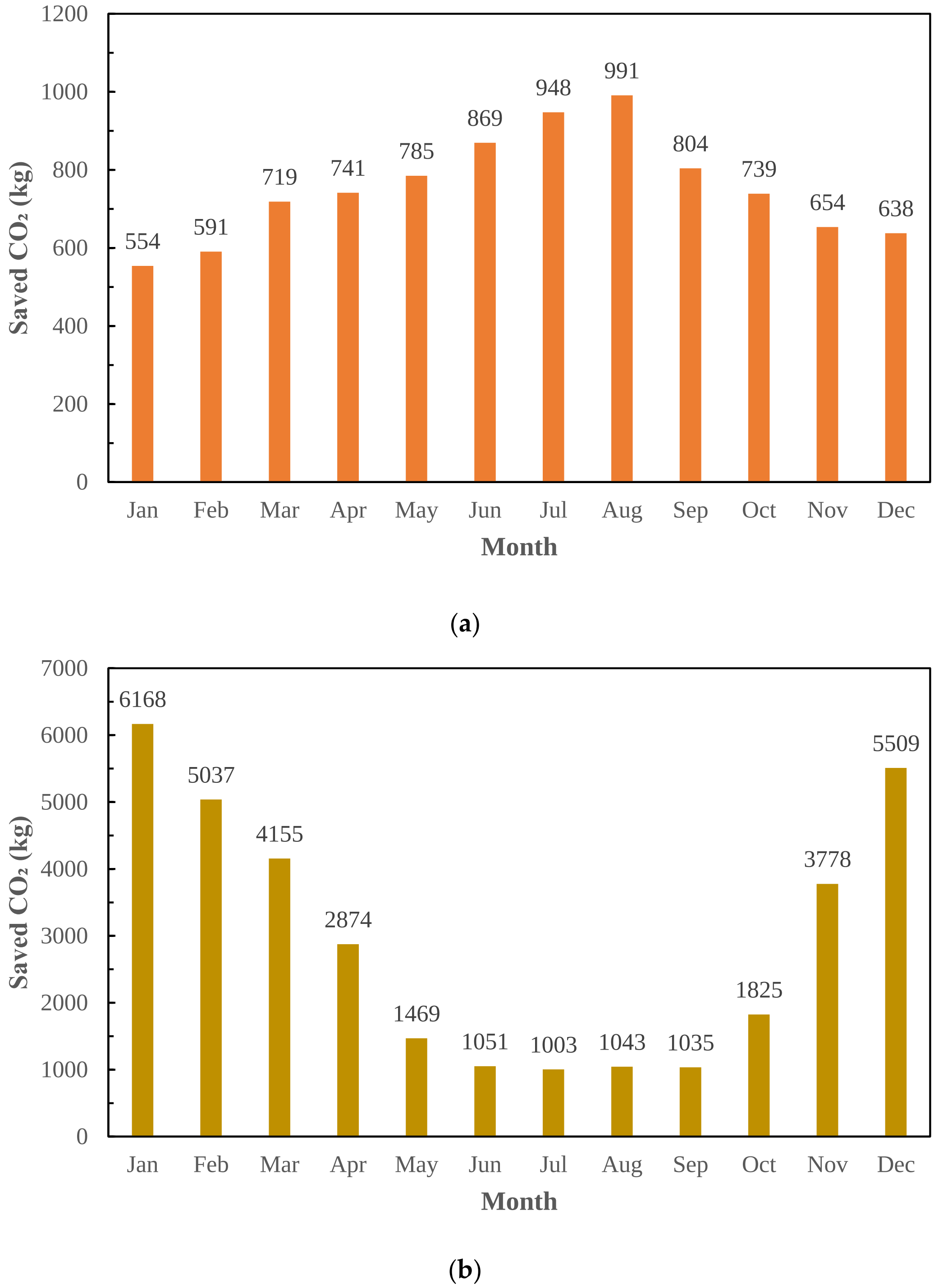

Figure 15. Monthly amount of SCD: (**a**) BIPV; (**b**) BIPVT.

Based on Figure 15a, in the BIPV system, in the months when power production is higher, the SCD also increases. Thus, the highest amount of SCD is 991 kg in August and the lowest amount is 554 kg in January. In Figure 15b, however, the trend is the opposite of Figure 15a, because there is no need for heat load in the hot months of the year, so as a result, the amount of SCD increases in the months that provide the highest heat load. As a result, the amount of carbon in January has the highest amount with 6168 kg and the lowest amount is in July with 1003 kg. Figure 16 shows the annual amount of SCD.

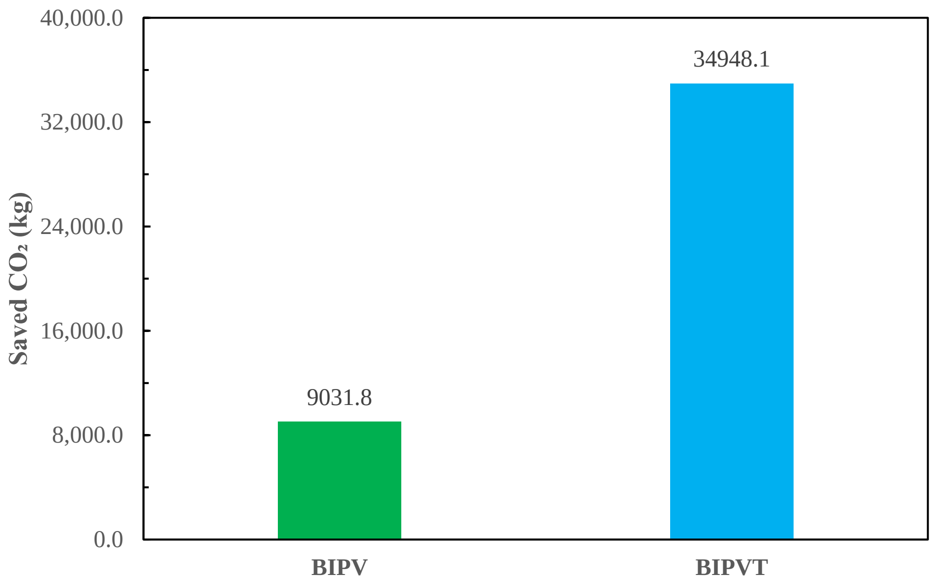

Figure 16. The yearly amount of SCD.

The annual amount of SCD in the BIPV system is equal to 9031.8 kg and in the BIPVT system is equal to 34,948.1 kg, which is a huge difference due to the provision of thermal load by the BIPVT system.

5. Conclusions

In the present study, the ability of a BIPV and BIPVT system to provide for the electrical and heating load of a residential building in cold weather conditions were compared from the perspectives of energy, exergy, economy, and environment. The studied city is Tabriz, which is located in the northwest of Iran. Unlike other systems that evaluated only a BIPV or BIPVT system, in this study, these two systems are evaluated from different perspectives to determine the performance of two systems in a cold city. From the point of view of energy, the BIPVT system produces 1.08 MWh of electrical energy in a year compared to the BIPV system and has the ability to supply 81.96 MWh of the building's thermal load. From an exergy point of view, by comparing the electrical efficiency in the BIPV system and the total efficiency in the BIPVT system, a difference of 1.69% is observed on average throughout the year. From the economic point of view, the PBT of the BIPV system is 5.77 years, while the PBT of the BIPVT system is 4.78 years due to producing higher electrical load and providing the heating load of the building. The amount of SCD in the BIPVT system is also 3.67 times compared to the BIPV system, which shows that the use of the BIPVT system in cold weather has a better performance compared to the BIPV system from the point of view of 4E.

This study considered Tabriz as a representative of a city with extremely cold winter and summer temperatures. Other climatic conditions have not been investigated in this study, and therefore, a comparative study between different cities could be carried out as a future work. In addition, one of the most common conditions for the design parameters was chosen and the calculations have been performed for this condition. The values for the effective parameters could be obtained through multi-objective optimization through another potential investigation as a further study.

Author Contributions: Conceptualization, R.J., M.H.S., A.S. and H.S.; methodology, R.J. and M.H.S.; software, R.J. and M.H.S.; validation, R.J. and M.H.S.; formal analysis, R.J. and M.H.S.; investigation, R.J.; writing—original draft preparation, R.J. and M.H.S.; writing—review and editing, A.S. and H.S.; visualization, R.J.; supervision, A.S. and H.S.; project administration, A.S. All authors have read and agreed to the published version of the manuscript.

Funding: This research received no external funding.

Data Availability Statement: Data will be available upon the request from the corresponding author. The data are not publicly available due to privacy.

Acknowledgments: The authors would like to sincerely thank the efforts of all members of Buildings journal who have been involved in processing this paper, including pre-submission, submission, and proofing stages. The authors would like to also acknowledge the valuable assistance provided by the AI language model from OpenAI in generating ideas and preliminary text for the motivation and literature review section of the introduction part of this manuscript. The content generated by the AI model served as a starting point and was subsequently reviewed, edited, and refined by the authors to align with the objectives and context of this publication. We affirm that all intellectual contributions have been made by the human authors in compliance with academic and ethical standards. Other parts of the work have all been completely written as the authors' original.

Conflicts of Interest: The authors declare no conflict of interest.

Nomenclature and Abbreviation

Nomenclature	
A	Area of PV (m^2)
Q	Rate of Heat (W)
c	Cost
c_p	Specific capacity $(\mathrm{J \cdot kg^{-1} \cdot K^{-1}})$
d	Interest rate (%)
E_x	Exergy (W)
D	Diameter (m)
G	Radiation $(\mathrm{W \cdot m^{-2}})$
i	Inflation rate (%)
k	Thermal conductivity $(\mathrm{W \cdot m^{-1} \cdot K^{-1}})$
P	Power (W)
V	speed $(\mathrm{m \cdot s^{-1}})$
R	Thermal resistance $(\mathrm{K} \cdot W^{-1})$
$\dot{m}$	Flow rate $(\mathrm{kg \cdot s^{-1}})$
T	Temperature (K)
t	Time (s)
Greek symbols	
α	Absorptivity
τ	Transmissivity
ε	Emissivity
η	Efficiency (%)
ρ	Density $(\mathrm{kg \cdot m^{-3}})$
β	Temperature coefficient of BIPV $(\% \cdot {}^\circ\mathrm{C}^{-1})$
δ	Thickness (m)
σ	Stefan Boltzmann $(\mathrm{W \cdot m^{-2} \cdot K^{-4}})$
Scripts	
a	Ambient
ac	Air Channel
c	Concrete
$cond$	Conduction
$conv$	Convection
db	Dry bulb
ele	electricity
$EVA1$	Top EVA
$EVA2$	Bottom EVA
g	Glass
h	Hydraulic
$inlet$	Inlet

NG	Natural gas
outlet	Outlet
om	Operating and maintenance
rad	Radiation
ref	Reference
Re	Reynolds Number
si	Silicon
sky	sky
sun	Sun
Td	Tedlar
th	thermal
w	wind
wb	Wet bulb
Abbreviation	
AGE	Annual Generated Electricity
AGH	Annual Generated Heat
BIPV	Building integrated Photovoltaic
EU	Europe
EVA	Ethylene Vinyl Acetate
GE	Generated Electricity
HR	Heat Recovery
BIPVT	Building integrated Photovoltaic thermal
IC	Initial Cost
LCA	Life Cycle Assessment
LHV	Low Heat Value
PBT	Payback Time
pcd	Produced carbon dioxide
PV	Photovoltaic
TE	Thermoelectric

References

1. Hoseinzadeh, S.; Groppi, D.; Sferra, A.S.; Di Matteo, U.; Astiaso Garcia, D. The PRISMI plus toolkit application to a grid-connected mediterranean island. *Energies* **2022**, *15*, 8652. [CrossRef]
2. Behrang, M.A.; Assareh, E.; Assari, M.R.; Ghanbarzadeh, A. Assessment of electricity demand in Iran's industrial sector using different intelligent optimization techniques. *Appl. Artif. Intell.* **2011**, *25*, 292–304. [CrossRef]
3. Maleki, Y.; Pourfayaz, F.; Mehrpooya, M. Experimental study of a novel hybrid photovoltaic/thermal and thermoelectric generators system with dual phase change materials. *Renew. Energy* **2022**, *201*, 202–215. [CrossRef]
4. Azizimehr, B.; Assareh, E.; Moltames, R. Thermoeconomic analysis and optimization of a solar micro CCHP by using TLBO algorithm for domestic application. *Energy Sources Part A Recovery Util. Environ. Eff.* **2020**, *42*, 1747–1761. [CrossRef]
5. Hoseinzadeh, S.; Nastasi, B.; Groppi, D.; Astiaso Garcia, D. Exploring the penetration of renewable energy at increasing the boundaries of the urban energy system—The PRISMI plus toolkit application to Monachil, Spain. *Sustain. Energy Technol. Assess.* **2022**, *54*, 102908. [CrossRef]
6. Khodayar Sahebi, H.; Hoseinzadeh, S.; Ghadamian, H.; Ghasemi, M.H.; Esmaeilion, F.; Garcia, D.A. Techno-economic analysis and new design of a photovoltaic power plant by a direct radiation amplification system. *Sustainability* **2021**, *13*, 11493. [CrossRef]
7. Groppi, D.; de Santoli, L.; Cumo, F.; Astiaso Garcia, D. A GIS-based model to assess buildings energy consumption and usable solar energy potential in urban areas. *Sustain. Cities Soc.* **2018**, *40*, 546–558. [CrossRef]
8. Karami, M.; Jalalizadeh, M. Performance comparison and risk assessment of BIPVT-based trigeneration systems using vapor compression and absorption chillers. *J. Build. Eng.* **2023**, *69*, 106244. [CrossRef]
9. Debbarma, M.; Sudhakar, K.; Baredar, P. Comparison of BIPV and BIPVT: A review. *Resour. Effic. Technol.* **2017**, *3*, 263–271. [CrossRef]
10. Debbarma, M.; Sudhakar, K.; Baredar, P. Thermal modeling, exergy analysis, performance of BIPV and BIPVT: A review. *Renew. Sustain. Energy Rev.* **2017**, *73*, 1276–1288. [CrossRef]
11. Gao, W.; Moayedi, H.; Shahsavar, A. The feasibility of genetic programming and ANFIS in prediction energetic performance of a building integrated photovoltaic thermal (BIPVT) system. *Sol. Energy* **2019**, *183*, 293–305. [CrossRef]
12. Jalalizadeh, M.; Fayaz, R.; Delfani, S.; Mosleh, H.J.; Karami, M. Dynamic simulation of a trigeneration system using an absorption cooling system and building integrated photovoltaic thermal solar collectors. *J. Build. Eng.* **2021**, *43*, 102482. [CrossRef]
13. Groppi, D.; Pfeifer, A.; Garcia, D.A.; Krajačić, G.; Duić, N. A review on energy storage and demand side management solutions in smart energy islands. *Renew. Sustain. Energy Rev.* **2021**, *135*, 110183. [CrossRef]

14. Cucumo, M.; Ferraro, V.; Kaliakatsos, D.; Nicoletti, F.; Gigliotti, A. A calculation model to estimate the electrical performance of a photovoltaic panel. *Tec. Ital.* **2021**, *65*, 256–263. [CrossRef]
15. Azam, M.W.; Chaudhary, G.Q.; Sajjad, U.; Abbas, N.; Yan, W.-M. Performance investigation of solar assisted desiccant integrated Maisotsenko cycle cooler in subtropical climate conditions. *Case Stud. Therm. Eng.* **2023**, *44*, 102864. [CrossRef]
16. Khanegah, M.R.; Ashrafizadeh, A.; Borooghani, D.; Torabi, F. Performance Evaluation of a Concentrated Photovoltaic/thermal System based on Water and Phase Change Material: Numerical Study and Experimental Validation. *Appl. Therm. Eng.* **2023**, *232*, 120936. [CrossRef]
17. Lamnatou, C.; Smyth, M.; Chemisana, D. Building-Integrated Photovoltaic/Thermal (BIPVT): LCA of a façade-integrated prototype and issues about human health, ecosystems, resources. *Sci. Total Environ.* **2019**, *660*, 1576–1592. [CrossRef] [PubMed]
18. Liu, Z.; Zhang, Y.; Yuan, X.; Liu, Y.; Xu, J.; Zhang, S.; He, B.-j. A comprehensive study of feasibility and applicability of building integrated photovoltaic (BIPV) systems in regions with high solar irradiance. *J. Clean. Prod.* **2021**, *307*, 127240. [CrossRef]
19. Rahmati Dehkordi, S.; Jahangiri, M. Sensitivity analysis for 3E assessment of BIPV system performance in Abadan in southwestern Iran. *J. Renew. Energy Environ.* **2022**, *9*, 1–12.
20. Gholami, H.; Nils Røstvik, H.; Steemers, K. The contribution of building-integrated photovoltaics (BIPV) to the concept of nearly zero-energy cities in Europe: Potential and challenges ahead. *Energies* **2021**, *14*, 6015. [CrossRef]
21. Shirazi, A.M.; Zomorodian, Z.S.; Tahsildoost, M. Techno-economic BIPV evaluation method in urban areas. *Renew. Energy* **2019**, *143*, 1235–1246. [CrossRef]
22. Kurz, D.; Głuchy, D.; Filipiak, M.; Ostrowski, D. Technical and Economic Analysis of the Use of Electricity Generated by a BIPV System for an Educational Establishment in Poland. *Energies* **2023**, *16*, 6603. [CrossRef]
23. Shakouri, M.; Ghadamian, H.; Noorpoor, A. Quasi-dynamic energy performance analysis of building integrated photovoltaic thermal double skin façade for middle eastern climate case. *Appl. Therm. Eng.* **2020**, *179*, 115724. [CrossRef]
24. Ibrahim, A.; Fudholi, A.; Sopian, K.; Othman, M.Y.; Ruslan, M.H. Efficiencies and improvement potential of building integrated photovoltaic thermal (BIPVT) system. *Energy Convers. Manag.* **2014**, *77*, 527–534. [CrossRef]
25. Dash, A.K.; Agrawal, S.; Gairola, S.; Shukla, S. Exergoeconomic and Envirnoeconomic Analysis of Building Integrated photovoltaic Thermal (BIPVT) System and its Optimization. *IOP Conf. Ser. Mater. Sci. Eng.* **2019**, *691*, 012078. [CrossRef]
26. Zhao, Y.; Li, W.; Zhang, G.; Li, Y.; Ge, M.; Wang, S. Experimental performance of air-type BIPVT systems under different climate conditions. *Sustain. Energy Technol. Assess.* **2023**, *60*, 103458. [CrossRef]
27. Shahsavar, A.; Talebizadehsardari, P.; Arıcı, M. Comparative energy, exergy, environmental, exergoeconomic, and enviroeconomic analysis of building integrated photovoltaic/thermal, earth-air heat exchanger, and hybrid systems. *J. Clean. Prod.* **2022**, *362*, 132510. [CrossRef]
28. Dash, A.K.; Agrawal, S.; Gairola, S.; Shukla, S. Analysis, Design, and Comparison of Different Building-Integrated Photovoltaic Thermal (BIPVT) System for Indian Meteorological Condition. In *Advances in Energy and Built Environment: Select Proceedings of TRACE 2018*; Springer: Singapore, 2020; pp. 145–157.
29. Ren, H.; Quan, Z.; Wang, Z.; Wang, L.; Jing, H.; Zhao, Y. Performance simulation and analysis of a multi-energy complementary energy supply system for a novel BIPVT nearly zero energy building. *Energy Convers. Manag.* **2023**, *282*, 116879. [CrossRef]
30. Bot, K.; Aelenei, L.; Gonçalves, H.; Gomes, M.d.G.; Silva, C.S. Performance assessment of a building-integrated photovoltaic thermal system in a mediterranean climate—An experimental analysis approach. *Energies* **2021**, *14*, 2191. [CrossRef]
31. Luo, Y.; Cheng, N.; Zhang, S.; Tian, Z.; Xu, G.; Yang, X.; Fan, J. Comprehensive energy, economic, environmental assessment of a building integrated photovoltaic-thermoelectric system with battery storage for net zero energy building. In *Building Simulation*; Tsinghua University Press: Beijing, China, 2022; pp. 1923–1941.
32. Shakouri, M.; Ghadamian, H.; Hoseinzadeh, S.; Sohani, A. Multi-objective 4E analysis for a building integrated photovoltaic thermal double skin Façade system. *Sol. Energy* **2022**, *233*, 408–420. [CrossRef]
33. Karami, R.; Sayyaadi, H. Optimal sizing of Stirling-CCHP systems for residential buildings at diverse climatic conditions. *Appl. Therm. Eng.* **2015**, *89*, 377–393. [CrossRef]
34. Shahverdian, M.H.; Sohani, A.; Pedram, M.Z.; Sayyaadi, H. An optimal strategy for application of photovoltaic-wind turbine with PEMEC-PEMFC hydrogen storage system based on techno-economic, environmental, and availability indicators. *J. Clean. Prod.* **2023**, *384*, 135499. [CrossRef]
35. Sohel, M.I.; Ma, Z.; Cooper, P.; Adams, J.; Scott, R. A dynamic model for air-based photovoltaic thermal systems working under real operating conditions. *Appl. Energy* **2014**, *132*, 216–225. [CrossRef]
36. Gu, W.; Ma, T.; Li, M.; Shen, L.; Zhang, Y. A coupled optical-electrical-thermal model of the bifacial photovoltaic module. *Appl. Energy* **2020**, *258*, 114075. [CrossRef]
37. Xu, L.; Luo, K.; Ji, J.; Yu, B.; Li, Z.; Huang, S. Study of a hybrid BIPV/T solar wall system. *Energy* **2020**, *193*, 116578. [CrossRef]
38. Nazri, N.S.; Fudholi, A.; Mustafa, W.; Yen, C.H.; Mohammad, M.; Ruslan, M.H.; Sopian, K. Exergy and improvement potential of hybrid photovoltaic thermal/thermoelectric (PVT/TE) air collector. *Renew. Sustain. Energy Rev.* **2019**, *111*, 132–144. [CrossRef]
39. Shahsavar, A.; Rajabi, Y. Exergoeconomic and enviroeconomic study of an air based building integrated photovoltaic/thermal (BIPV/T) system. *Energy* **2018**, *144*, 877–886. [CrossRef]
40. Sohani, A.; Sayyaadi, H.; Miremadi, S.R.; Yang, X.; Doranehgard, M.H.; Nizetic, S. Determination of the best air space value for installation of a PV façade technology based on 4E characteristics. *Energy* **2023**, *262*, 125386. [CrossRef]

41. Gu, W.; Ma, T.; Shen, L.; Li, M.; Zhang, Y.; Zhang, W. Coupled electrical-thermal modelling of photovoltaic modules under dynamic conditions. *Energy* **2019**, *188*, 116043. [CrossRef]
42. Shahsavar, A.; Arıcı, M. Effect of glass cover on the energy and exergy performance of a combined system including a building integrated photovoltaic/thermal system and a sensible rotary heat exchanger. *Int. J. Energy Res.* **2022**, *46*, 5050–5066. [CrossRef]
43. Li, Z.X.; Shahsavar, A.; Al-Rashed, A.A.A.A.; Kalbasi, R.; Afrand, M.; Talebizadehsardari, P. Multi-objective energy and exergy optimization of different configurations of hybrid earth-air heat exchanger and building integrated photovoltaic/thermal system. *Energy Convers. Manag.* **2019**, *195*, 1098–1110. [CrossRef]
44. Amirhaeri, Y.; Pourfayaz, F.; Hadavi, H.; Kasaeian, A. Energy and exergy analysis-based monthly co-optimization of a polygeneration system for power, heating, cooling, and hydrogen production. *J. Therm. Anal. Calorim.* **2023**, *148*, 8195–8221. [CrossRef]
45. Buonomano, A.; Calise, F.; Palombo, A.; Vicidomini, M. Transient analysis, exergy and thermo-economic modelling of façade integrated photovoltaic/thermal solar collectors. *Renew. Energy* **2019**, *137*, 109–126. [CrossRef]
46. Ramadhani, F.; Hussain, M.A.; Mokhlis, H.; Illias, H.A. Optimal heat recovery using photovoltaic thermal and thermoelectric generator for solid oxide fuel cell-based polygeneration system: Techno-economic and environmental assessments. *Appl. Therm. Eng.* **2020**, *181*, 116015. [CrossRef]